© 1982 The Chemical Society of Japan Bull. Chem. Soc. Jpn., 55, 3004—3012 (1982) [Vol. 55, No. 9

Catalytic Efficiency of Functionalized Vesicles in the Transamination of Pyridoxal-5′-phosphate with a Hydrophobic Amino Acid[†]

Yukito Murakami,* Akio Nakano, and Kazunari Akiyoshi
Department of Organic Synthesis, Faculty of Engineering, Kyushu University,
Hakozaki, Higashi-ku, Fukuoka 812

(Received April 13, 1982)

The transamination reaction of pyridoxal-5′-phosphate (PLP) with *N*-dodecyl-L-alaninamide ($AlaC_{12}$) was investigated in an aqueous phosphate–borate buffer at pH 7.0, μ 0.10 (KCl), and 30.0±0.1 °C in the presence of single-walled vesicles of *N,N*-ditetradecyl-N^{α}-(6-trimethylammoniohexanoyl)-L-histidinamide bromide ($N^+C_5His2C_{14}$). The electrostatic and hydrophobic interactions between the vesicles and the reactants resulted in incorporation of PLP and $AlaC_{12}$ into polar and hydrophobic domains of the vesicles, respectively, in the Schiff-base formation process. The isomerization of the aldimine Schiff-base to the corresponding ketimine Schiff-base was confirmed to be the rate-determining step in the transamination process. The reaction site in the vesicular system was found to be equivalent in polarity to dioxane–water (7:3 v/v). However, the overall reaction rate in the vesicles was enhanced 230-fold relative to that in dioxane–water (7:3 v/v). A hydrophobic and suitably polar microenvironment constructed at the reaction site is responsible for such a marked rate-enhancement. In addition, each vesicle of $N^+C_5His2C_{14}$ provided functional (imidazolyl) groups in its hydrogen-belt domain to catalyze the intramolecular prototropic shift to yield the ketimine Schiff-base. The microenvironmental effects of molecular assemblies of *N,N*-ditetradecyl-N^{α}-(6-trimethylammoniohexanoyl)-L-alaninamide bromide and CTAB on the overall transamination were also discussed.

Although the apoproteins in vitamin B_6-dependent enzymes play essential roles not only in rate enhancement but also in substrate-recognition and reaction specificity which leads to selective cleavage of the covalent bonds around the α-carbon atom of a substrate,[1] the mechanistic details as regards such functions have not been fully understood up to the present time. These functions may be characterized tentatively as follows: (1) each apoprotein provides a hydrophobic environment in its interior region in which pyridoxal-5′-phosphate is buried; (2) it catalyzes a specific reaction by its various functional groups such as the imidazolyl group of histidine and the ε-amino group of lysine; (3) it constructs a hydrophobic cavity, shape and size of which are specific to its substrate, so that the substrate-selectivity is exercised; (4) such a hydrophobic cavity fixes its specific substrate in space to carry out the desired reaction. On these grounds, micellar surfactants,[2,3] synthetic polymers,[4] and macrocyclic compounds[5,6] have been developed to simulate the functions of vitamin B_6-dependent enzymes.

We have recently reported that amphiphiles involving an amino acid residue interposed between a polar head group and an aliphatic double-chain form stable single-compartment vesicles in aqueous media due to formation of the hydrogen-belt region in the intramembrane region.[7] These amphiphiles were confirmed to construct three characteristic domains in their vesicular aggregates; a polar surface domain composed of charged head groups, semipolar barrier domain composed of amino acid residues (so-called hydrogen belt), and a hydrophobic interior domain composed of aliphatic double-chains. Thus, these various domains may be utilized as reaction site models of the apoenzymes, specific to the nature of reactants. In the present study, the transamination reaction of pyridoxal-5′-phosphate (PLP) with *N*-dodecyl-L-alaninamide ($AlaC_{12}$), a hydrophobic amino acid analogue, in the presence of single-walled vesicles of $N^+C_5His2C_{14}$ and $N^+C_5Ala2C_{14}$ as well as in the presence of CTAB micelles. The microenvironmental effects provided by these cationic amphiphiles on the transamination reaction have been characterized.

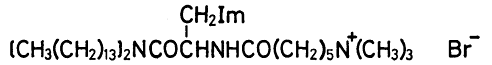

$$[CH_3(CH_2)_{13}]_2NCO\overset{CH_2Im}{\overset{|}{C}}HNHCO(CH_2)_5\overset{+}{N}(CH_3)_3\quad Br^-$$

$N^+C_5His2C_{14}$ (Im: Imidazolyl)

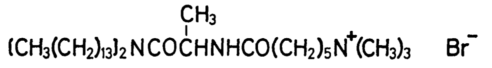

$$[CH_3(CH_2)_{13}]_2NCO\overset{CH_3}{\overset{|}{C}}HNHCO(CH_2)_5\overset{+}{N}(CH_3)_3\quad Br^-$$

$N^+C_5Ala2C_{14}$

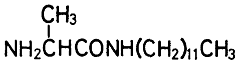

$$NH_2\overset{CH_3}{\overset{|}{C}}HCONH(CH_2)_{11}CH_3$$

$AlaC_{12}$

$CH_3(CH_2)_{15}\overset{+}{N}(CH_3)_3\quad Br^-$

CTAB

Experimental

Spectroscopic data were taken on a JASCO DS-403G grating IR spectrophotometer, a Hitachi Perkin-Elmer R-20 NMR spectrometer, a Union Giken SM-401 high-sensitivity UV-visible spectrophotometer, and a Hitachi 650—60 fluorescence spectrophotometer. pH-Measurements were carried out with a Beckman expandomatic SS-2 pH meter equipped with a Metrohm EA-125 combined electrode after calibration with a combination of appropriate standard aqueous buffers. Melting points were measured with a Yanagimoto MP-S1 apparatus (hot-plate type).

Hexadecyltrimethylammonium bromide (CTAB) of Nakarai Chemicals was recrystallized from ethanol, mp 237—239 °C (decomp). Dodecylamine of Nakarai Chemicals was distilled under reduced pressure, bp 95—98 °C/266 Pa. Pyridoxamine-5′-phosphate (PMP: Calbiochem, U.S.A.; A-grade), pyridoxal hydrochloride (PL: Mann Research Laboratories, U.S.A.), and pyridoxal-5′-phosphate (PLP: Nakarai Chemicals; bio-analytical grade) were used without further purification. *N*-Dodecyl-L-alaninamide ($AlaC_{12}$) was prepar-

---

[†] Contribution No. 661 from this Department.

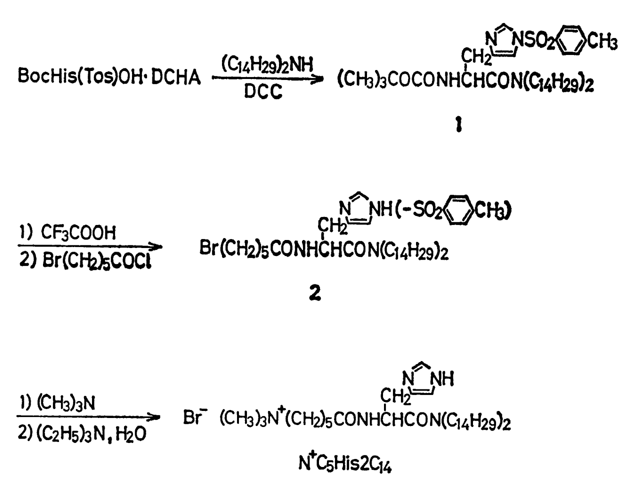

(Boc, *t*-butoxycarbonyl; Tos, tosyl; DCHA, dicyclohexylamine)

Scheme 1.

ed by condensation of *t*-butoxycarbonyl-L-alanine with dodecylamine in the presence of dicyclohexylcarbodiimide (DCC), followed by elimination of the *t*-butoxycarbonyl group with hydroformic acid. The product was recrystallized from diethyl ether to give a white solid, mp 51—52 °C. Found: C, 69.78; H, 12.38; N, 10.81%. Calcd for $C_{15}H_{32}N_2O$: C, 70.26; H, 12.58; N, 10.92%. *N*,*N*-Ditetradecyl-*N*$^\alpha$-(6-trimethylammoniohexanoyl)-L-alaninamide bromide ($N^+C_5Ala2C_{14}$) was synthesized in a manner similar to that reported previously for the preparation of *N*,*N*-didodecyl-*N*$^\alpha$-(6-trimethylammoniohexanoyl)-L-alaninamide bromide,[7d)] and characterized as reported elsewhere.[7f)]

The synthetic procedure for *N*,*N*-ditetradecyl-*N*$^\alpha$-(6-trimethylammoniohexanoyl)-L-histidinamide bromide (N^+C_5-$His2C_{14}$) is outlined in Scheme 1.

N,N-*Ditetradecyl*-N$^\alpha$-t-*butoxycarbonyl*-N^{im}-*tosyl*-L-*histidinamide (1).* To a solution of the dicyclohexylamine adduct of *N*$^\alpha$-*t*-butoxycarbonyl-*N*^{im}-tosyl-L-histidine (5.0 g, 8.5 mmol)[8)] in dry dichloromethane (40 ml) was added *p*-toluenesulfonic acid (1.7 g, 8.8 mmol) in 5 min with stirring at room temperature. After *N*,*N*-ditetradecylamine (3.4 g, 8.8 mmol) and dicyclohexylcarbodiimide (1.85 g, 8.9 mmol) were added to the reaction mixture in this order at room temperature and 0 °C, respectively, the mixture was stirred for 3 h at 0 °C and for 12 h at room temperature. The resulting precipitates (*N*,*N*′-dicyclohexylurea) were removed by filtration, the solvent was evaporated *in vacuo*, and the residual oil was dissolved in ethyl acetate (150 ml). The solution was then washed with 10% aqueous citric acid, saturated aqueous sodium chloride, 4% aqueous sodium hydrogencarbonate, and saturated sodium chloride in this sequence. After being dried over Na_2SO_4, the mixture was evaporated *in vacuo* to afford an oil which was subsequently purified by centrifugal liquid chromatography with a combination of silica gel (Wako gel B-5) and chloroform; a pale yellow oil which was solidified in a refrigerator, yield 5.6 g (83%). IR (neat): 3200 (NH str.), 2840 and 2800 (CH str.), 1705 and 1625 (C=O str.) cm^{-1}. NMR ($CDCl_3$, TMS): δ 0.88 [6H, broad t, $C\underline{H}_3(CH_2)_{13}$–], 1.24 [48H, s, $CH_3(C\underline{H}_2)_{12}$-$CH_2$–], 1.34 [9H, s, $(CH_3)_3COCO$–], 2.40 (3H, s, –SO_2C_6-$H_4C\underline{H}_3$), 2.80 [2H, d, –$CH(C\underline{H}_2$Im-Tos)], 3.12 [4H, broad t, $CH_3(CH_2)_{12}C\underline{H}_2N$–], 4.75 (1H, broad q, –CH–), 5.20 (1H, d, NH), 6.98 (1H, s, Im-5H), 7.80 (1H, s, Im-2H), 7.23 (2H, d, tosyl's 3H and 5H), and 7.74 (2H, d, tosyl's 2H and 6H).

N,N-*Ditetradecyl*-N$^\alpha$-*(6-bromohexanoyl)*-L-*histidinamide (2).* Trifluoroacetic acid (6 g, 53 mmol) was added to a dichloromethane solution (10 ml) of **1** (1.9 g, 2.4 mmol), and the mixture was stirred for 1.5 h at room temperature. Evaporation of an excess amount of trifluoroacetic acid *in vacuo* below 40 °C gave a pale brown oil (**1a**). Elimination of the *t*-butoxycarbonyl group was confirmed by NMR spectroscopy. The amine (**1a**) was dissolved in dry dichloromethane (5 ml) and the solution was cooled to 0 °C. Triethylamine (3.4 g, 34 mmol) was added dropwise to the solution, and then 6-bromohexanoyl chloride (1.0 g, 4.7 mmol) dissolved in dry dichloromethane (10 ml) was added dropwise to the mixture at 0 °C with stirring. The resulting mixture was stirred for 2.5 h at 0 °C and then washed with 4% aqueous citric acid, saturated aqueous sodium chloride, 4% aqueous sodium hydrogencarbonate, and saturated aqueous sodium chloride in this sequence. After being dried over Na_2SO_4, the solution was evaporated *in vacuo* to give a pale brown oil; yield 1.6 g (93%). A major fraction of the tosyl group was eliminated as confirmed by NMR spectroscopy. The product was used for the subsequent reaction without further purification. NMR ($CDCl_3$, TMS): δ 0.87 [6H, broad t, $C\underline{H}_3(CH_2)_{13}$–], 1.25 [48H, s, $CH_3(C\underline{H}_2)_{12}$-$CH_2$–], ~2.00 [6H, m, $BrCH_2(C\underline{H}_2)_3CH_2CO$–], 2.35 [2H, broad t, $Br(CH_2)_4C\underline{H}_2CO$–], 2.80 (2H, d, –$CHC\underline{H}_2$Im–), 3.35 [2H, t, $BrC\underline{H}_2(CH_2)_4CO$–], 3.00—3.40 [4H, m, CH_3-$(CH_2)_{12}C\underline{H}_2N$–], 5.05 (1H, broad q, –CH–), 6.45 (1H, d, NH), 7.15 (1H, s, Im-5H), and 7.94 (1H, s, Im-2H).

N,N-*Ditetradecyl*-N$^\alpha$-*(6-trimethylammoniohexanoyl)*-L-*histidinamide Bromide* ($N^+C_5His2C_{14}$). Dry trimethylamine gas was introduced into a benzene solution (30 ml) of **2** (1.6 g, 2.2 mmol) for 1.5 h to reach the gas saturation level, and the solution was stirred at room temperature for 12 h. The solvent was evaporated off *in vacuo*, and the residual oil was dissolved in benzene–acetone (36 ml, 5:1 v/v). To the solution was added 30% aqueous triethylamine (2 ml) with stirring at room temperature to eliminate the tosyl group completely. After the resulting solution was stirred for 3.5 h, the solvent was evaporated off *in vacuo*. The crude product was purified by gel-filtration chromatography on columns of Sephadex LH-20 and Toyopearl HW-40 in this sequence with methanol as an eluant: a white glassy solid, yield 0.32 g (19%); mp 182 °C, $[\alpha]^{20}_D$ −14.2° (*c* 1.13, ethanol). IR (neat): 3280 (NH, OH str.) and 1630 (C=O str.) cm^{-1}. NMR ($CDCl_3$, TMS): δ 0.85 [6H, broad t, $C\underline{H}_3(CH_2)_{13}$–], 1.22 [48H, s, $CH_3(C\underline{H}_2)_{12}CH_2$–], ~1.90 [6H, m, $N^+CH_2(C\underline{H}_2)_3$-$CH_2CO$–], 2.32 [2H, broad t, $N^+(CH_2)_4C\underline{H}_2CO$–], 2.80—3.62 [8H, m, $CH_3(CH_2)_{12}C\underline{H}_2N$–, $N^+C\underline{H}_2(CH_2)_4CO$–, and –$CHC\underline{H}_2$Im–], 3.35 [9H, s, $(CH_3)_3N^+$–], 5.05 (1H, broad q, $NHC\underline{H}CO$–), 6.90 (1H, s, Im-5H), 7.62 (1H, d, NH), and 7.95 (1H, s, Im-2H). Found: C, 63.99; H, 10.58; N, 8.58%. Calcd for $C_{43}H_{84}N_5BrO_2\cdot(3/2)H_2O$: C, 63.75; H, 10.82; N, 8.65%.

Kinetic Measurements. An amount of pyridoxamine-5′-phosphate formed in the transamination reaction was determined by measuring a fluorescence intensity at the emission maximum of PMP excited at 328 nm. Each run was initiated by adding 50 µl of an aqueous solution of PLP (1.02×10^{-3} mol dm^{-3}) and 40 µl of an ethanol solution of *N*-dodecyl-L-alaninamide (1.99×10^{-2} mol dm^{-3}) to 2.00 ml of a reaction medium which was pre-equilibrated at 30.0±0.1 °C in a thermostated cell set in the fluorescence spectrophotometer. The reaction medium was prepared as follows; (1) an appropriate amount of the stock solution of an amphiphile in ethanol was placed in a glass vessel, ethanol was removed *in vacuo*, and 10 ml of the aqueous buffer (6.23 mmol dm^{-3} phosphate–1.88 mmol dm^{-3} borate, pH 7.0) containing 0.1

mol dm^{-3} potassium chloride was added to the residue; (2) the aqueous dispersion of an amphiphile thus prepared was sonicated for 4 min with a probe-type sonicator at 30-W power (W-220F, Heat Systems-Ultrasonics). The resulting vesicle solution was sufficiently clear without noticeable turbidity and gave good kinetic reproducibility. Kinetic measurements in aqueous dioxane were carried out under similar conditions. Light was emitted to an experimental solution only at the instant of each fluorescence intensity measurement.

Electron Microscopy. Both aqueous dispersion (A) and ultrasonicated aqueous solution (B) of $N^+C_5His2C_{14}$ were employed for the measurements. As sample A, 16 mg of $N^+C_5His2C_{14}$ was suspended in 2 ml of deionized and distilled water containing 2%(w/w) uranyl acetate and the dispersion was shaked occasionally and heated until the glassy solid disappeared completely to give slightly turbid dispersion. As sample B, an aqueous dispersion of $N^+C_5His2C_{14}$ (sample A) was sonicated for 4 min with a probe-type sonicator at 30-W power and allowed to stand for 10 min at 5 °C. A clear solution was then obtained. Samples A and B were applied on carbon grids and dried in a vacuum desiccator. A JEOL JEM-200B electron microscope, installed at the Research Laboratory of High Voltage Electron Microscope of our University, was used for the measurements. Electron micrographs for $N^+C_5His2C_{14}$ are shown in Fig. 1, while those for $N^+C_5Ala2C_{14}$ have been reported elsewhere.[7f)] Both multiwalled vesicles and lamellae were observed in an electron micrograph of the aqueous dispersion as shown in Fig. 1. On the other hand, the sonicated aqueous solution showed exclusively the formation of single-walled vesicles. Similar patterns of electron micrographs have been observed for respective samples of $N^+C_5Ala2C_{14}$. The present amphiphiles were used in the state of single-walled vesicles for study.

Differential Scanning Calorimetry (DSC). Each 50-μl sample of an aqueous dispersion of the amphiphile [2.0% (w/w)] in an aqueous buffer of 6.23 mmol dm^{-3} phosphate–1.88 mmol dm^{-3} borate, containing 0.1 mol dm^{-3} potassium chloride, was sealed up in a silver sample cell. The measurements were made on a differential scanning calorimeter (Daini Seikosha SSC-560U): heating rate, 0.5 °C/min; sensitivity, 0.025 mcal/s/(full scale); chart speed, 0.5 cm/min. The obtained calorimetric parameters for the amphiphiles are as follows, where T_m represents a temperature at a peak maximum of DSC thermogram.

$N^+C_5Ala2C_{14}$: T_m, 2.0 °C; ΔH, 20.5 kJ mol^{-1}

$N^+C_5His2C_{14}$: T_m, 2.5 °C; ΔH, 19.2 kJ mol^{-1}

Results and Discussion

The transamination reaction of pyridoxal-5′-phosphate (PLP) with $AlaC_{12}$ in the presence of an amphiphile was followed by electronic spectroscopy in an aqueous phosphate–borate buffer at pH 7.0, μ 0.10 (KCl), and 30.0±0.1 °C. Figure 2 shows the spectral change observed along the progress of transamination in the presence of $N^+C_5His2C_{14}$ vesicles. The spectral change shows that the reaction is consistent with a two-step mechanism. The first step, which reached an equilibrium stage within 4 min, was followed by a comparatively slow step. The isosbestic points associated with the respective steps are as follows: first, 312 and 357 nm; second, 292 and 345 nm. A half-life for the second slow step is several hours. Absorption spectra observed at the final stages of the respective steps showed that the first step is referred to the Schiff-base formation and the second one to the formation of pyridoxamine-5′-phosphate (PMP). The absorption spectrum observed at the final stage of the first step showed maxima at 338 and 415 nm, and is the typical one for a pyridoxylideneamino acid formed with PLP.[9)] The absorption spectrum observed at the final stage of the second step, having maxima at 253 and 328 nm, is identical with that of PMP.[10)] The absorption spectrum, which can be attributed to the corresponding ketimine Schiff-base (λ_{max} 310—330 nm),[9)] was not detected in the course of the second step. A similar spectral behavior

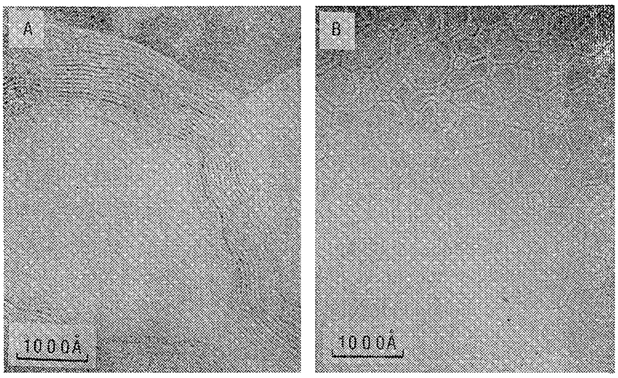

Fig. 1. Electron micrographs for $N^+C_5His2C_{14}$ negatively stained with uranyl acetate: A, 10 mmol dm^{-3} aqueous dispersion (magnification, ×92 000); B, 10 mmol dm^{-3} aqueous solution sonicated for 4 min at 30-W power and subsequently allowed to stand for 10 min at 5 °C (magnification, ×92 000).

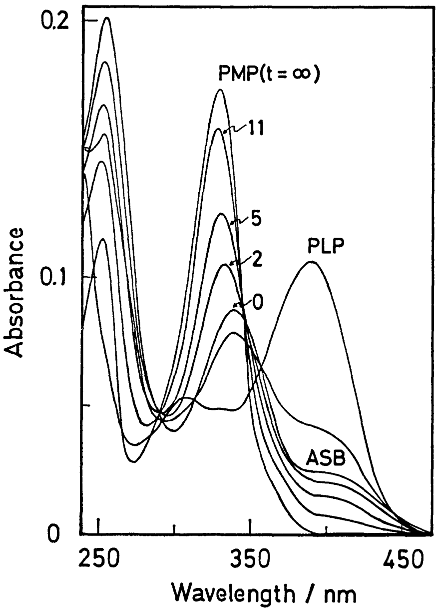

Fig. 2. Spectral change along the progress of reaction of PLP (2.44×10^{-5} mol dm^{-3}) with $AlaC_{12}$ (3.81×10^{-4} mol dm^{-3}) in the presence of $N^+C_5His2C_{14}$ (9.7×10^{-4} mol dm^{-3}) in aqueous phosphate (6.0 mmol dm^{-3})–borate (1.8 mmol dm^{-3}), containing 1.9%(v/v) ethanol, at pH 7.0, μ 0.1 (KCl), and 30.0±0.1 °C. Numerals refer to reaction times (in h) for the second slow step.

TABLE 1. EQUILIBRIUM CONSTANTS AND SPECTRAL PARAMETERS FOR THE SCHIFF-BASE FORMATION BETWEEN PLP AND $AlaC_{12}$ IN VARIOUS MEDIA AT 30.0±0.1 °C[a)]

Medium	Dioxane-Water (42:58 v/v)	Dioxane-Water (7:3 v/v)	CTAB	$N^+C_5Ala2C_{14}$	$N^+C_5His2C_{14}$
λ_{max}^{PLP}/nm	380	380[b)]	389	389	389
$\varepsilon_\lambda{}^{PLP}$	3.4×10^3	2.6×10^3 [b)]	4.4×10^3	4.4×10^3	4.4×10^3
$\varepsilon_\lambda{}^{ASB}$	1400	910	550	740	840
K_{SB}/mol^{-1} dm^3 [c)]	1.1×10^4	2.7×10^4	3.1×10^5	8.6×10^4	1.5×10^5

a) Cationic amphiphile systems: in aqueous phosphate (6.0 mmol dm^{-3})-borate (1.8 mmol dm^{-3}) containing 1.9% (v/v) ethanol at pH 7.0 and μ 0.1 (KCl); CTAB, 2.9×10^{-3} mol dm^{-3}; $N^+C_5Ala2C_{14}$, 9.7×10^{-4} mol dm^{-3}; $N^+C_5His2C_{14}$, 9.7×10^{-4} mol dm^{-3}. Dioxane-water (42:58 v/v): dioxane containing 58%(v/v) aqueous buffer (6.2 mmol dm^{-3} phosphate, 1.8 mmol dm^{-3} borate, and 0.1 mol dm^{-3} potassium chloride) and 1.9%(v/v) ethanol. Dioxane-water (7:3 v/v): dioxane containing 30%(v/v) aqueous buffer (6.2 mmol dm^{-3} phosphate, 1.8 mmol dm^{-3} borate, and 0.1 mol dm^{-3} potassium chloride) and 1.9%(v/v) ethanol. b) Wavelength and molar extinction coefficient of PLP employed for calculation of [ASB] in order to achieve accuracy of spectral analysis, while $\lambda_{max}=370$ nm and $\varepsilon^{PLP}(370\text{ nm})=4.1\times10^3$. c) Cationic amphiphile systems: PLP, 4.93×10^{-5} mol dm^{-3}; $AlaC_{12}$, 4.90×10^{-5} mol dm^{-3}. Dioxane-water (7:3 v/v): PLP, 4.90×10^{-5} mol dm^{-3}; $AlaC_{12}$, 9.80×10^{-5} mol dm^{-3}. Dioxane-water (42:58 v/v): PLP, 4.85×10^{-5} mol dm^{-3}; $AlaC_{12}$, 3.88×10^{-4} mol dm^{-3}.

along the progress of reaction was observed in other amphiphile systems. In the light of these observations, the overall reaction pathway is explicitly given by Eq. 1.

$$PLP + AlaC_{12} \underset{\text{fast}}{\overset{K_{SB}}{\rightleftharpoons}} ASB \underset{\text{slow}}{\overset{k_{AK}}{\rightleftharpoons}} KSB \xrightarrow{\text{very fast}} PMP + PyC_{12} \qquad (1)$$

Here, ASB, KSB, and PyC_{12} refer to the aldimine Schiff-base, the ketimine Schiff-base, and *N*-dodecylpyruvinamide, respectively. Thus, the rate determining step for the present transamination reaction is the isomerization of the aldimine Schiff-base (ASB) to the corresponding ketimine Schiff-base (KSB). This finding is consistent with the results obtained in PLP-dependent transamination reactions both in an enzyme system[11)] and model systems.[12)] The present two reaction steps were treated separately since the respective rates were much different from each other.

Schiff-base Formation. In order to clarify microenvironmental effects on the aldimine Schiff-base formation, the equilibrium constants (K_{SB}) for the first step were determined in the presence and absence of the cationic amphiphiles. The equilibrium constant, as defined by Eq. 2, for the Schiff-base formation between PLP and $AlaC_{12}$ was evaluated as follows.

$$K_{SB} = \frac{[ASB]}{[PLP][AlaC_{12}]} \qquad (2)$$

This is rearranged to give Eq. 3.

$$K_{SB} = \frac{[ASB]}{(T_P-[ASB])(T_A-[ASB])} \qquad (3)$$

Here, T_P and T_A refer to total concentrations of PLP and $AlaC_{12}$, respectively. An absorbance (A_λ) at the absorption maximum of PLP (λ, 389 and 380 nm in molecular assemblies of the cationic amphiphiles and aqueous dioxane, respectively) is represented by Eq. 4.

$$A_\lambda = \varepsilon_\lambda{}^{PLP}(T_P-[ASB]) + \varepsilon_\lambda{}^{ASB}[ASB] \qquad (4)$$

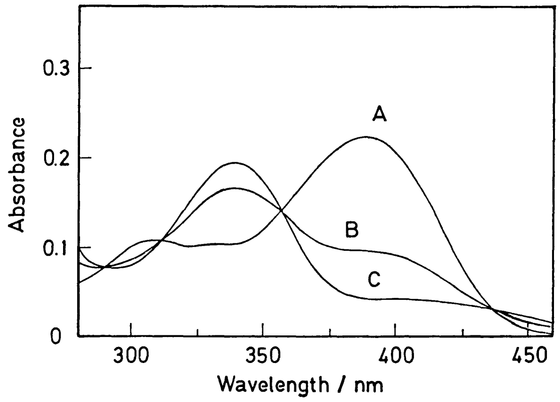

Fig. 3. Absorption spectra for the aldimine Schiff-base system of PLP (4.93×10^{-5} mol dm^{-3}) with varying amounts of $AlaC_{12}$ (A, 0; B, 4.90×10^{-5}; C, 3.86×10^{-4} mol dm^{-3}) in the presence of $N^+C_5His2C_{14}$ (9.7×10^{-4} mol dm^{-3}) in aqueous phosphate (6.0 mmol dm^{-3})-borate (1.8 mmol dm^{-3}), containing 1.9% (v/v) ethanol, at pH 7.0, μ 0.1 (KCl), and 30.0±0.1 °C.

Here, $\varepsilon_\lambda{}^{PLP}$ and $\varepsilon_\lambda{}^{ASB}$ are molar extinction coefficients of PLP and ASB observed at the absorption maximum of PLP, respectively. Then, Eq. 4 is rearranged to Eq. 5. The value of $\varepsilon_\lambda{}^{ASB}$ was evaluated directly

$$[ASB] = \frac{\varepsilon_\lambda{}^{PLP}T_P - A_\lambda}{\varepsilon_\lambda{}^{PLP} - \varepsilon_\lambda{}^{ASB}} \qquad (5)$$

from the spectrum observed in the presence of a large excess of $AlaC_{12}$; a complete conversion of PLP into the Schiff-base is assured under such conditions. Figure 3 shows the absorption spectra of the PLP–$AlaC_{12}$ system involving varying amounts of $AlaC_{12}$ in the presence of $N^+C_5His2C_{14}$. For a complete conversion of PLP into the aldimine Schiff-base, only a small excess of $AlaC_{12}$ (*ca.* 11 fold) over PLP was needed in the vesicular and micellar systems. On the other hand, over a 90-fold excess of $AlaC_{12}$ was required in aqueous dioxane to complete the conversion. The formation constants thus determined and the relevant spectral parameters in molecular assemblies of the cationic amphiphiles and in aqueous dioxane are listed in Table 1.

TABLE 2. EQUILIBRIUM CONSTANTS AND SPECTRAL PARAMETERS FOR TWO ALDIMINE SCHIFF-BASES (SB_1 AND SB_2) IN VARIOUS MEDIA AT 30.0 ± 0.1 °C[a)]

	Dioxane-Water[b)]					CTAB	$N^+C_5Ala2C_{14}$	$N^+C_5His2C_{14}$
	10	20	30	39	48			
$\lambda_{SB_1}/nm^{c)}$	338	338	338	338	338	338	338	338
$\lambda_{SB_2}/nm^{d)}$	420	420	420	420	420	415	415	415
K_α	37.2	16.2	10.4	8.2	6.5	19.9	10.9	10.4

a) Cationic amphiphile systems: in aqueous phosphate (6.0 mmol dm^{-3})-borate (1.8 mmol dm^{-3}) containing 1.9% (v/v) ethanol at pH 7.0 and μ 0.1 (KCl); CTAB, 2.9×10^{-3} mol dm^{-3}; $N^+C_5Ala2C_{14}$, 9.7×10^{-4} mol dm^{-3}; $N^+C_5His2C_{14}$, 9.7×10^{-4} mol dm^{-3}; PLP, 4.93×10^{-5} mol dm^{-3}; $AlaC_{12}$, 3.86×10^{-4} mol dm^{-3}. Dioxane-water mixtures: each medium was prepared by mixing dioxane with aqueous buffer (6.2 mmol dm^{-3} phosphate, 1.8 mmol dm^{-3} borate, and 0.1 mol dm^{-3} potassium chloride); PLP, $(4.72—4.83)\times10^{-5}$ mol dm^{-3}; $AlaC_{12}$, $(2.42—4.72)\times10^{-3}$ mol dm^{-3}. b) Numerals refer to the content of aqueous buffer in %(v/v). c) ε_{SB_1}, 4.6×10^3. d) ε_{SB_2}, 9.4×10^3.

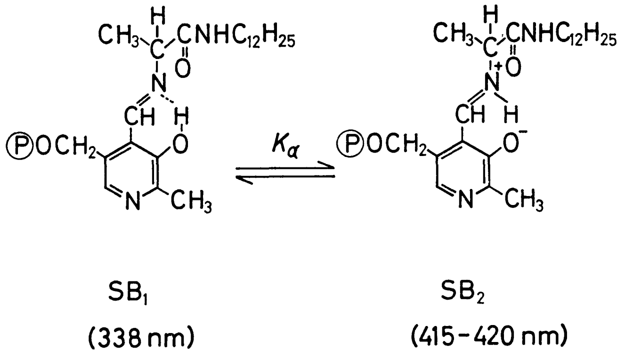

Ⓟ: A phosphate group.

Scheme 2.

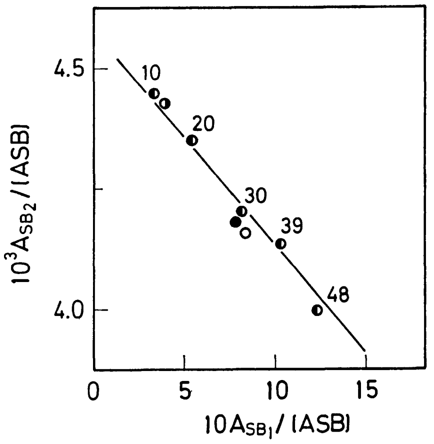

Fig. 4. Plot of $A_{SB_1}/[ASB]$ vs. $A_{SB_2}/[ASB]$ for equilibrium of aldimine Schiff-base species of PLP and $AlaC_{12}$ (SB_1 and SB_2) in dioxane–water mixtures (◐) and cationic amphiphile systems: $N^+C_5His2C_{14}$ (○), $N^+C_5Ala2C_{14}$ (●), and CTAB (◑). Numerals refer to the water contents in aqueous dioxane. See Table 2 for experimental conditions.

The microenvironments constructed with the amphiphiles, into which the Schiff-base was incorporated, were characterized in terms of an equilibrium constant (K_α) defined by Eq. 6 on the following basis. An absorption spectrum of the aldimine Schiff-base showed the presence of two species in an equilibrium state (Fig. 3). They differ from each other in the protonation site as shown in Scheme 2. The neutral form (SB_1) with an ordinary amino acid was primarily observed in hydrophobic environments constructed with such components as organic solvents,[9)] aqueous micelles,[13)] reversed micelles,[3)] and alkylamines bearing a long hydrocarbon chain.[14,15)] The charged form (SB_2), on the other hand, was found exclusively in aqueous media.[16)] These two species of the aldimine Schiff-base are in an equilibrium which is highly dependent on the microenvironmental polarity. The equilibrium constant between SB_1 and SB_2 is, therefore, referred to an efficient polarity parameter for characterization of the microenvironment to which the Schiff-base is bound.

$$K_\alpha = \frac{[SB_1]}{[SB_2]} = \frac{A_{SB_1}/\varepsilon_{SB_1}}{A_{SB_2}/\varepsilon_{SB_2}} \qquad (6)$$

Here, A_{SB_1} and A_{SB_2} refer to absorbances observed at the absorption maxima of SB_1 and SB_2 species, respectively; ε_{SB_1} and ε_{SB_2} stand for molar extinction coefficients of SB_1 and SB_2 species at their absorption maxima, respectively. These values were determined according to the reported method employed for evaluation of those values for the Schiff-base of PLP with hexylamine.[15)] Equation 7 can be derived on the basis of Scheme 2, where [ASB] refers to a total concentration of SB_1 and SB_2, and is equal to a PLP concentration employed under the conditions that PLP is completely converted into the Schiff-base ($[PLP]\ll[AlaC_{12}]$).

$$A_{SB_1}/[ASB] = \varepsilon_{SB_1} - (\varepsilon_{SB_1}/\varepsilon_{SB_2})(A_{SB_2}/[ASB]) \qquad (7)$$

The plot of $A_{SB_1}/[ASB]$ vs. $A_{SB_2}/[ASB]$ for the Schiff-base of PLP with $AlaC_{12}$ in aqueous dioxane resulted in a good linear relationship ($r>0.993$) as shown in Fig. 4. The data obtained in molecular assemblies of the cationic amphiphiles are also plotted in Fig. 4 and found along the correlation line for the dioxane–water system. The K_α-values thus obtained are summarized in Table 2, together with the relevant spectral parameters. Since the solvent-polarity parameter (Kosower's Z-value)[17)] can be correlated with the standard Gibbs free energy ($\Delta G^0 = -RT\ln K_\alpha$),[15)] we estimated the microenvironmental polarity of the reaction site for the Schiff-base formation in the light of a linear relation shown in Fig. 5. The result indicates that the reaction sites in the vesicular and micellar systems are equivalent in polarity to dioxane–water (7:3 v/v) and dioxane–water (8:2 v/v), respectively. The reaction sites in the vesicular systems are more polar than that in the micellar system, most likely due to the presence of the hydrogen belt domain in the former. The hydrogen belt region divides the vesicular system into hydrophobic and polar domains,[7c)] and PLP of hydrophilic nature is entrapped in the polar domain. The hydrophobic and less polar microenvironment provided by CTAB micelles is in favor of the Schiff-base formation relative to the polar reaction sites by the vesicular systems. The interaction modes of the reactants (PLP and $AlaC_{12}$) with the cationic aggregates were further examined on the basis of the following experimental facts. (1) The absorption maximum of PLP observed in the presence of the cationic aggregates (micelles and vesicles) was identical with that without those if $AlaC_{12}$ was absent. (2) The Schiff-base was not detected spectrophotometrically with a small excess of $AlaC_{12}$ over pyridoxal (PL), which has no phosphate group, in the cationic aggregates. (3) Formation of the Schiff-base of PLP with $AlaC_{12}$ was suppressed at higher ionic strength [μ=1.0 (KCl)]. (4) A large excess of an amino acid (L-alanine) was required to detect formation of the Schiff-base with PLP even in the presence of the cationic aggregates. (5) Without any cationic amphiphile, the content of dioxane in reaction media must exceed 40%(v/v) to investigate the Schiff-base formation between PLP and $AlaC_{12}$ because of the insolubility of $AlaC_{12}$ in water.

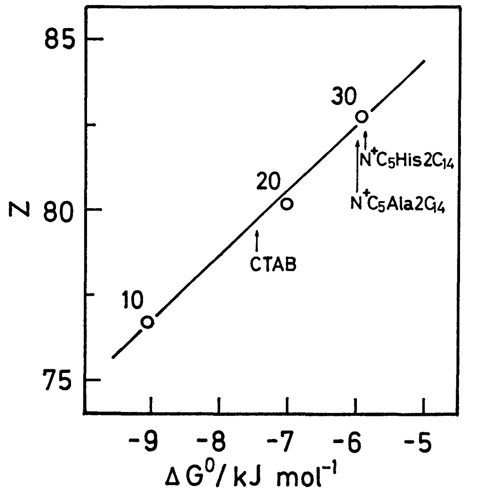

Fig. 5. Correlation of ΔG^0 with solvent polarity parameter (Z). Numerals refer to the water contents in aqueous dioxane. ΔG^0-Values for cationic amphiphile systems are shown by arrows.

These results indicate that PLP is concentrated at the surface area of the cationic aggregates due to the electrostatic interaction between the anionic phosphate group of PLP and the cationic head group of the amphiphile employed, while $AlaC_{12}$ is incorporated into the hydrophobic domain of the aggregates through mutual hydrophobic interaction. Consequently, both electrostatic and hydrophobic interactions play important roles in the Schiff-base formation in the presence of the amphiphile aggregates. The Schiff-base formation step in the present vesicular system is schematically shown in Fig. 6.

Transamination Reaction. The overall transamination reaction of PLP was followed by means of fluorescence spectroscopy at 30.0±0.1 °C in the presence and absence of cationic amphiphiles. The reaction was examined under the conditions of $[AlaC_{12}] \gg [PLP]$; PLP was converted completely into the aldimine Schiff-base within 4 min. The reaction, for which the isomerization of the aldimine Schiff-base to the corresponding ketimine Schiff-base becomes rate-determining as mentioned above, was followed after complete formation of the aldimine Schiff-base. The fluorescence intensity at specified wavelengths (cationic aggregates, 393 nm; dioxane–water 405 nm) increased gradually along the progress of the reaction (Fig. 7). When a pseudo-substrate (1-dodecylamine) was used in place of $AlaC_{12}$, the fluorescence intensity remained unchanged. Table 3 summarizes the excitation wavelengths of PLP and PMP and the corresponding relative emission intensities in the presence and absence of the cationic amphiphiles. The fluorescence quantum yield of the Schiff-base was negligibly low compared with that of PMP.[14)] The PMP concentration in the reaction system was determined on the basis

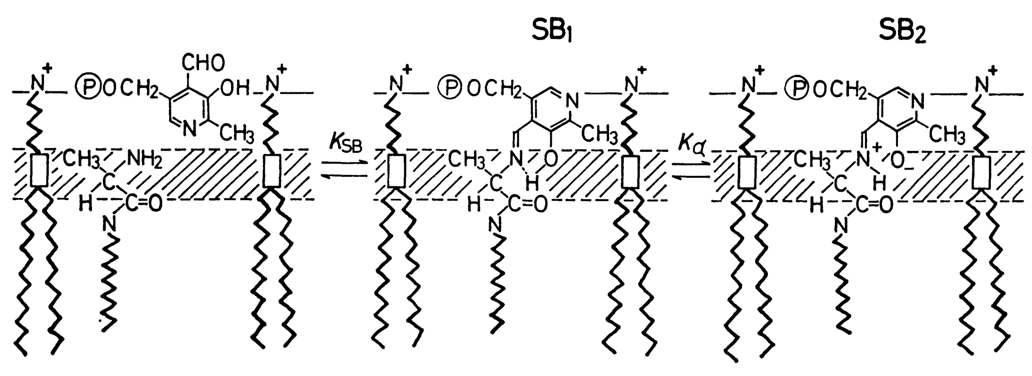

Fig. 6. Schematic representation of the Schiff-base formation step in vesicular phase: a rectangle, an amino acid residue; Ⓟ, a phosphate group. A shaded portion refers to the hydrogen belt region, which has some hydrophobic and polar nature, and to the reaction site for the overall transamination process.

TABLE 3. FLUORESCENCE MAXIMA (λ_F), RELATIVE EMISSION INTENSITIES (I_{rel}), AND EXCITATION WAVELENGTHS (λ_E) FOR PLP AND PMP IN VARIOUS MEDIA AT 30.0±0.1 °C[a)]

Medium	PLP			PMP		
	λ_F/nm	λ_E/nm	I_{rel}[b)]	λ_F/nm	λ_E/nm	I_{rel}[b)]
Aqueous buffer[c)]	500	395	1.0	394	328	1250
Aqueous dioxane[d)]	532	390	4.3	405	333	343
CTAB[e)]	500	389	1.7	394	328	770
$N^+C_5Ala2C_{14}$[e)]	504	389	2.0	393	328	687
$N^+C_5His2C_{14}$[e)]	480	389	2.0	393	328	673

a) Fluorescence maxima in the absence of $AlaC_{12}$; concentrations of PLP and PMP, 2.44×10^{-5} mol dm^{-3}. b) Relative emission intensity with reference to the intensity for PLP in aqueous buffer. c) Aqueous phosphate (6.2 mmol dm^{-3})-borate (1.8 mmol dm^{-3}), containing 0.1 mol dm^{-3} potassium chloride (pH 7.0). d) Dioxane containing 30%(v/v) aqueous buffer (6.2 mmol dm^{-3} phosphate, 1.8 mmol dm^{-3} borate, and 0.1 mol dm^{-3} potassium chloride). e) In aqueous phosphate (6.1 mmol dm^{-3})-borate (1.8 mmol dm^{-3}) at pH 7.0 and μ 0.1 (KCl); CTAB, 2.9×10^{-3} mol dm^{-3}; $N^+C_5Ala2C_{14}$, 9.8×10^{-4} mol dm^{-3}; $N^+C_5His2C_{14}$, 9.8×10^{-4} mol dm^{-3}.

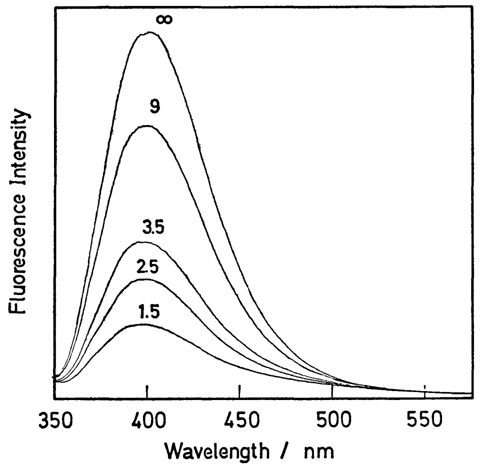

Fig. 7. Fluorescence-spectral change along the progress of reaction of PLP (2.44×10^{-5} mol dm^{-3}) with $AlaC_{12}$ (3.81×10^{-4} mol dm^{-3}) in the presence of $N^+C_5His2C_{14}$ (9.7×10^{-4} mol dm^{-3}) in aqueous phosphate (6.0 mmol dm^{-3})-borate (1.8 mmol dm^{-3}), containing 1.9%(v/v) ethanol, at pH 7.0, μ 0.1 (KCl), and 30.0±0.1 °C. Numerals refer to reaction times (in h) for the second slow step.

of Eq. 8 by measuring a fluorescence intensity (I_t) at appropriate time intervals.[18)]

$$\frac{I_t}{I_0}=\frac{C^t_{PMP}}{C^0_{PMP}}\times 10^{-0.5[(C^t_{PMP}-C^0_{PMP})\varepsilon_{PMP}+\varepsilon_{SB}C^t_{SB}]}\,. \tag{8}$$

Here, I_0 is a fluorescence intensity of PMP at its known concentration (C^0_{PMP}) in the absence of other reacting species; ε_{PMP} and ε_{SB} are molar extinction coefficients of PMP and the aldimine Schiff-base at a specified excitation wavelength, respectively; C^t_{PMP} and C^t_{SB} refer to concentrations of PMP and the aldimine Schiff-base observed at time t (s) after complete formation of the Schiff-base. C^t_{SB} is related with C^0_{SB} and C^t_{PMP} by Eq. 9, where C^0_{SB} refers to an initial concentration of the aldimine Schiff-base in the isomerization process and is equal to the PLP concentration used here (C^0_{PLP}).

$$C^t_{SB}=C^0_{SB}-C^t_{PMP} \tag{9}$$

The correlations between C^t_{PMP} and time are shown in Fig. 8. The rate equation for PMP formation is given by Eq. 10 in reference to Eq. 1, which is subsequently integrated to give Eq. 11.

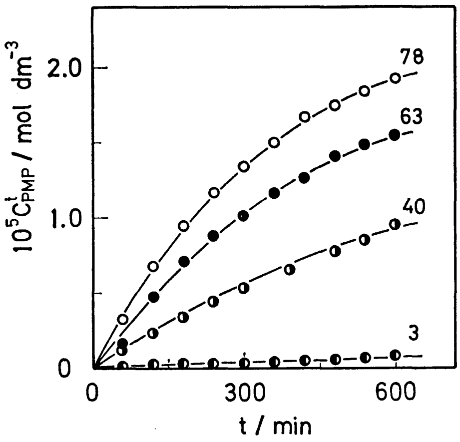

Fig. 8. Time-courses of PMP formation for transamination of PLP with $AlaC_{12}$ in aqueous dioxane (◐) and cationic amphiphile systems: $N^+C_5His2C_{14}$ (○), $N^+C_5Ala2C_{14}$ (●), and CTAB (◑). Numerals represent rates of conversion of PLP into PMP at t=600 min. See Table 4 for experimental conditions.

$$\frac{dC_{PMP}}{dt}=-k_{AK}C^t_{SB}=-k_{AK}(C^0_{PLP}-C^t_{PMP}) \tag{10}$$

$$\ln\frac{C^0_{PLP}}{(C^0_{PLP}-C^t_{PMP})}=k_{AK}\cdot t \tag{11}$$

In each case, a good linear relationship between the left hand term of Eq. 11 and reaction time t was obtained as shown in Fig. 9 (r>0.998). The reaction was followed for 10 h and the first-order kinetics were found to hold in each kinetic run. The conversion rates of PLP to PMP at the ends of such kinetic runs (after 10 h) were determined as shown in Fig. 8. Under the conditions employed in this work, the reversed reaction from PMP to the aldimine Schiff-base was not detected. The rate constants for the isomerization process are summarized in Table 4, along with the overall second-order rate constants ($K_{SB}\cdot k_{AK}$) and relative effectiveness (k_{rel}) of the reac-

Table 4. Kinetic parameters for transamination in various media at 30.0±0.1 °C[a)]

Medium	Aqueous dioxane	CTAB	$N^+C_5Ala2C_{14}$	$N^+C_5His2C_{14}$
k_{AK}/s^{-1}	1.0×10^{-7}	1.3×10^{-6}	2.7×10^{-6}	4.2×10^{-6}
$K_{SB}\cdot k_{AK}/mol^{-1}\,dm^3\,s^{-1}$	2.7×10^{-3}	4.0×10^{-1}	2.3×10^{-1}	6.3×10^{-1}
k_{rel}[b)]	1	148	85	233

a) Cationic amphiphile systems: in aqueous phosphate (6.0 mmol dm^{-3})-borate (1.8 mmol dm^{-3}) containing 1.9% (v/v) ethanol at pH 7.0 and μ 0.1 (KCl); CTAB, 2.9×10^{-3} mol dm^{-3}; $N^+C_5Ala2C_{14}$, 9.7×10^{-4} mol dm^{-3}; $N^+C_5His2C_{14}$, 9.7×10^{-4} mol dm^{-3}; PLP, 2.44×10^{-5} mol dm^{-3}; $AlaC_{12}$, 3.81×10^{-4} mol dm^{-3}. Aqueous dioxane: dioxane containing 30%(v/v) aqueous buffer (6.2 mmol dm^{-3} phosphate, 1.8 mmol dm^{-3} borate, and 0.1 mol dm^{-3} potassium chloride) and 1.9%(v/v) ethanol; PLP, 2.44×10^{-5} mol dm^{-3}; $AlaC_{12}$, 1.23×10^{-3} mol dm^{-3}. b) Relative rate, taking $K_{SB}\cdot k_{AK}$ in aqueous dioxane as a reference.

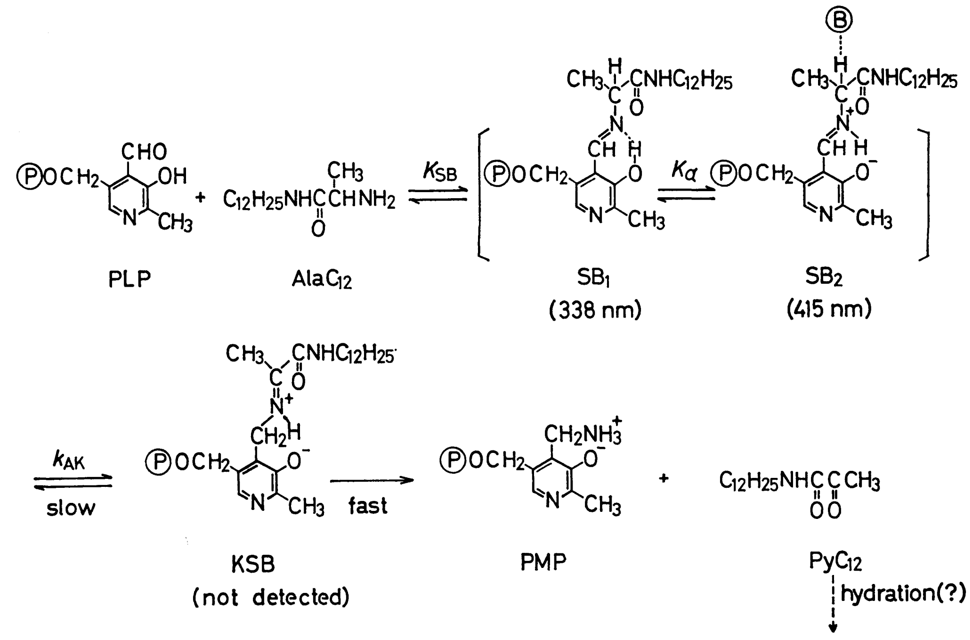

Ⓑ: A hydroxide ion and/or an imidazolyl group.
Ⓟ: A phosphate group.

Scheme 3.

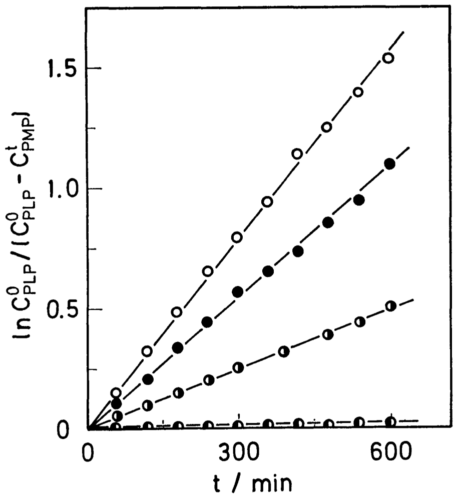

Fig. 9. Analysis of kinetic data (Fig. 8) on the basis of Eq. 11.

tion media.

The rate-determining step in the transamination reaction investigated here is referred to the isomerization of the aldimine Schiff-base to the ketimine one, since the accumulation of the latter was not detected spectrophotometrically in the course of the reaction. This means that the deprotonation from the α-carbon of the amino acid moiety is essential for the transamination, and such apparent intramolecular proton-transfer to afford the ketimine Schiff-base becomes rate-determining. The reaction was much accelerated in the cationic aggregate systems as compared with that in dioxane–water mixtures. This suggests that the concentration of hydroxide ion becomes efficient on the surface area of the cationic aggregates and is one of the important factors for rate enhancement as often observed in cationic micellar catalysis.[19)] Secondly, the increase in a fraction of the active aldimine Schiff-base (SB_2), which is controlled by the microenvironmental property acted on the Schiff-base, is responsible for the rate acceleration. The fractions of the active SB_2 species in the whole aldimine Schiff-base were calculated with reference to K_α-values; 5 and 9% in the micellar and vesicular systems, respectively. Such difference reflects the microenvironmental property of reaction sites. Formation of the polar SB_2 species is favored in a polar microenvironment. Thirdly, the imidazolyl group placed at the reaction site is in favor of the rate enhancement. The $N^+C_5His2C_{14}$ vesicles enhanced the reaction by more than 1.5 fold relative to the $N^+C_5Ala2C_{14}$ vesicles, even though the former may provide a microenvironment similar to that with the latter as mentioned above. The neutral imidazolyl group may act as a general-base catalyst which promotes the prototropic shift in a manner as observed for the imidazole-catalyzed transamination of α-aminophenylacetic acid.[12b] The overall transamination between PLP and $AlaC_{12}$ in the $N^+C_5His2C_{14}$ vesicles is now plausibly explained by Scheme 3.

In conclusion, a hydrophobic and polar microenvironment accelerates the overall transamination more than a hydrophobic but less polar one, even though the Schiff-base formation is more enhanced in the latter. The bilayer vesicles having an amino acid residue as a molecular component may provide better microenvironments for the transamination than ordinary micelles. This suggests that the hydrogen belt domain constructed in the vesicular assembly may be characterized as a suitable model for reaction sites in enzymes.[20] The vesicles formed with N^+C_5-$His2C_{14}$ provide functional groups in the hydrogen belt domain to catalyze the intramolecular prototropic shift and can be taken as a functionalized apoenzyme model for vitamin B_6-dependent enzymes

References

1) a) K. G. Scrimgeour, "Chemistry and Control of Enzyme Reactions" Academic Press, New York (1977), Chap. 8; b) H. C. Dunathan, *Adv. Enzymol.*, **35**, 79 (1971).

2) Y. Murakami and H. Kondo, *Bull. Chem. Soc. Jpn.*, **48**, 541 (1975).

3) H. Kondo, H. Yoshinaga, and J. Sunamoto, *Chem. Lett.*, **1980**, 973.

4) Y. N. Belokon', V. I. Tararov, T. F. Savel'eva, and V. M. Belikov, *Makromol. Chem.*, **181**, 2183 (1980).

5) R. Breslow, M. Hammond, and M. Lauer, *J. Am. Chem. Soc.*, **102**, 421 (1980).

6) H. Kuzuhara, T. Komatsu, and S. Emoto, *Tetrahedron Lett.*, **1978**, 3563.

7) a) Y. Murakami, A. Nakano, and K. Fukuya, *J. Am. Chem. Soc.*, **102**, 4253 (1980); b) Y. Murakami, A. Nakano, A. Yoshimatsu, and K. Fukuya, *ibid.*, **103**, 728 (1981); c) Y. Murakami, Y. Aoyama, A. Nakano, T. Tada, and K. Fukuya, *ibid.*, **103**, 3951 (1981); d) Y. Murakami, A. Nakano, and H. Ikeda, *J. Org. Chem.*, **47**, 2137 (1982); e) Y. Murakami, Y. Aoyama, J. Kikuchil K. Nishida, and A. Nakano, *J. Am. Chem. Soc.*, **104**, 2937 (1982); f) Y. Murakami, A. Nakano, and A. Yoshimatsu, *ibid.*, submitted for publication.

8) The dicyclohexylamine adduct of N^{α}-*t*-butoxycarbonyl-N^{im}-tosyl-L-histidine was prepared in reference to the procedure reported by Fujii *et al*; mp 159—161 °C (lit, 160—162 °C): T. Fujii and S. Sakakibara, *Bull. Chem. Soc. Jpn.*, **47**, 3146 (1974).

9) Y. Matsushima and A. E. Martell, *J. Am. Chem. Soc.*, **89**, 1322 (1967).

10) The product analysis for the reaction of PLP (1.0×10^{-4} mol dm^{-3}) with $AlaC_{12}$ (1.0×10^{-4} mol dm^{-3}), which lasted 5 d at room temperature, was carried out by paper chromatography [Toyo filter paper No. 50, 1-propanol–aqueous ammonia (28%)–water (7:1:2 v/v) as an eluant, ninhydrin or iodide test for detection]. The result clearly indicated the disappearance of $AlaC_{12}$ along with the formation of PMP in the course of the reaction, while the formation of *N*-dodecylpyruvinamide was not detected.

11) G. G. Hammes and P. Fasella, *J. Am. Chem. Soc.*, **84**, 4644 (1962).

12) a) A. E. Braunstein, "The Enzymes," 2nd ed, ed by P. D. Boyer, H. Lardy, and K. Mirbäck, Academic Press, New York (1960), Vol. 2, pp. 113—181; b) T. C. Bruice and R. M. Topping, *J. Am. Chem. Soc.*, **85**, 1480 (1963).

13) V. Gani, A. Kupfer, and S. Shaltiel, *Biochemistry*, **17**, 1294 (1978).

14) K. O. Honikel and N. B. Madsen, *J. Biol. Chem.*, **247**, 1057 (1972).

15) J. Llor and M. Cortijo, *J. Chem. Soc., Perkin Trans. 2*, **1977**, 1111.

16) D. E. Metzler, *J. Am. Chem. Soc.*, **79**, 485 (1957).

17) E. M. Kosower, *J. Am. Chem. Soc.*, **80**, 3253 (1958).

18) T. Förster, "Fluoreszenz Organischer Verbindungen," Vandenhoeck & Ruprecht, Göttingen (1951).

19) J. H. Fendler and E. J. Fendler, "Catalysis in Micellar and Macromolecular Systems," Academic Press, New York (1975).

20) D. E. Metzler, *Adv. Enzymol.*, **50**, 1 (1979).